Genetic Architecture Associated With Familial Short Stature

Ying-Ju Lin,[1,2] Chi-Fung Cheng,[1,3] Chung-Hsing Wang,[4] Wen-Miin Liang,[3] Chih-Hsin Tang,[5] Li-Ping Tsai,[6] Chien-Hsiun Chen,[2,7] Jer-Yuarn Wu,[2,7] Ai-Ru Hsieh,[8] Ming Ta Michael Lee,[9] Ting-Hsu Lin,[1] Chiu-Chu Liao,[1] Shao-Mei Huang,[1] Yanfei Zhang,[9] Chang-Hai Tsai,[10] and Fuu-Jen Tsai,[1,2,4,10]

[1]Genetic Center, Department of Medical Research, China Medical University Hospital, Taichung 40447, Taiwan; [2]School of Chinese Medicine, China Medical University, Taichung 40402, Taiwan; [3]Department of Health Services Administration, China Medical University, Taichung 40402, Taiwan; [4]Children's Hospital of China Medical University, Taichung 40447, Taiwan; [5]Graduate Institute of Biomedical Sciences, China Medical University, Taichung 40402, Taiwan; [6]Department of Pediatrics, Taipei Tzu Chi Hospital, New Taipei City, 23142, Taiwan; [7]Institute of Biomedical Sciences, Academia Sinica, Taipei 11529, Taiwan; [8]Department of Statistics, Tamkang University, New Taipei City 25137, Taiwan; [9]Genomic Medicine Institute, Geisinger, Danville, Pennsylvania 17822, USA and [10]Department of Biotechnology and Bioinformatics, Asia University, Taichung 41354, Taiwan.

ORCiD number: 0000-0003-2267-7058 (Y.-J. Lin).

Context: Human height is an inheritable, polygenic trait under complex and multilocus genetic regulation. Familial short stature (FSS; also called genetic short stature) is the most common type of short stature and is insufficiently known.

Objective: To investigate the FSS genetic profile and develop a polygenic risk predisposition score for FSS risk prediction.

Design and Setting: The FSS participant group of Han Chinese ancestry was diagnosed by pediatric endocrinologists in Taiwan.

Patients and Interventions: The genetic profiles of 1163 participants with FSS were identified by using a bootstrapping subsampling and genome-wide association studies (GWAS) method.

Main Outcome Measures: Genetic profile, polygenic risk predisposition score for risk prediction.

Results: Ten novel genetic single nucleotide polymorphisms (SNPs) and 9 reported GWAS human height-related SNPs were identified for FSS risk. These 10 novel SNPs served as a polygenic risk predisposition score for FSS risk prediction (area under the curve: 0.940 in the testing group). This FSS polygenic risk predisposition score was also associated with the height reduction regression tendency in the general population.

Conclusion: A polygenic risk predisposition score composed of 10 genetic SNPs is useful for FSS risk prediction and the height reduction tendency. Thus, it might contribute to FSS risk in the Han Chinese population from Taiwan. **(*J Clin Endocrinol Metab* 105: 1801–1813, 2020)**

Freeform/Key Words: familial short stature, polygenic trait, human height, Han Chinese ancestry, GWAS

ISSN Print 0021-972X ISSN Online 1945-7197
Printed in USA

Received 9 October 2019. Accepted 10 March 2020.
First Published Online 14 March 2020.
Corrected and Typeset 11 April 2020.

Abbreviations: AUC, area under the curve; CI, confidence interval; FSS, familial short stature; GWAS, genome-wide association studies; GH, growth hormone; IGF-1, insulin-like growth factor; LD, linkage disequilibrium; OR, odds ratio; ROC, receiver operating characteristic; SNP, single nucleotide polymorphism.

Human height is an inheritable, polygenic trait under complex and multilocus genetic regulation (1–3). Genetic predisposition to human height has been widely explored using genome-wide association studies (GWAS) in multi-ethnic populations (4–14). Among these studies, approximately 700 single nucleotide polymorphisms (SNPs) in 420 genetic loci were reported. These genetic loci were associated with tyrosine phosphatase family proteins, insulin-like growth factor, skeletal development, mitosis, fibroblast growth factors, Wnt/β-catenin pathway, hedgehog signaling, and cancer-associated pathways, among others, highlighting the polygenic nature of human height.

Short stature is defined as a body height less than the third percentile or less than 2 standard deviations below the mean height for the corresponding age and gender according to the growth standards for height of the population (15). Bone homeostasis is a physiological process and the balance between bone remodeling and bone formation (16). Bone homeostasis is also a cellular physiological process with osteoclastogenesis and osteogenesis maintained by osteoclasts and chondrocytes, respectively (17). Osteoclasts and chondrocytes play important roles in the growth plate as well as in human height regulation (18, 19). The role of bone homeostasis in short stature remains to be elucidated. In addition, familial short stature (FSS; also called genetic short stature) is the most common type of short stature and is only caused by genetic factors (20–22). However, the genetic profile for FSS and its molecular influence in bone biology remains to be investigated (1).

In this study, we investigated the genetic predisposition to FSS in Han Chinese people in Taiwan using a bootstrapping subsampling and GWAS method (23, 24). We found 10 novel and 9 human height GWAS-reported SNPs robustly associated with FSS risk. A height reduction regression tendency in the general population was also observed between cumulative genetic predisposition score and human height regardless of gender.

Participants and Methods

Ethics and consent

This study is a cross-sectional study on the clinical, biochemical, and genetic findings collected from participants with FSS sequentially identified from the Children's Hospital, China Medical University, Taichung, Taiwan, from August 1999 to September 2018. This study was approved by the institutional review board and the ethics committee of the Human Studies Committee of China Medical University Hospital. Written informed consent was obtained from the participants, their parents, or legal guardians according to institutional requirements and Declaration of Helsinki principles (25).

Participants

The participant group used in this study was diagnosed by pediatric endocrinologists in Taiwan (Fig. 1 and Supplementary Fig. S1) All supplementary material and figures are located in a digital research materials repository (26). The participant group included a cohort with FSS (N = 1163). All recruited participants were of Han Chinese ancestry and diagnosed with FSS (1, 20, 22). The selection criteria for FSS was (1) (a) height less than the third percentile (Supplementary Fig. 7) (2, 26), (b) (father and/or mother) less than the third percentile (3), (c) bone age appropriate for chronologic age (4), (d) normal onset of puberty (5), (e)normal annual growth rate, and (6) (f) normal results of clinical biochemistry examination. Excluded individuals were those with all other abnormal morphology and karyotyping results, abnormal bone age or puberty stage, or abnormal serum or plasma levels of clinical biochemistry examinations for growth hormone–insulin-like growth factor 1(GH-IGF1) axis, thyroid function, or precocious puberty (Supplementary Fig. S1) (26). There were 1163 participants with FSS in the current study.

In this study, the control group consisted of 4168 individuals from the Taiwan Biobank (TW-Biobank; http://www.twbiobank.org.tw/new_web/index.php) and our type 2 diabetes cohorts (Fig. 1 and Supplementary Fig. 6) (26). Furthermore, the selection criteria for control groups (N = 1071) were (1) height exceeding the 75th percentile for age and gender of the general population in Taiwan, (2) no history of FSS, and (3) age < 61 years. All participant and control groups in this study were of Han Chinese origin based on principal component analysis of genome-wide data (Supplementary Fig. S2) (26).

Genotyping and quality control

Genomic deoxyribonucleic acid was extracted from the blood samples of participants according to standard protocols using the Qiagen genomic deoxyribonucleic acid isolation kit (Qiagen, Taichung, Taiwan). Each participant with FSS (N = 1163) was genotyped at the National Genotyping Centre at Academia Sinica (Taipei, Taiwan) using the Axiom genome-wide CHB array plate, according to the manufacturer's procedure. For the control group from the Taiwan Biobank, the GWAS data of each sample was genotyped using the Axiom genome-wide TWB array plate. For the control

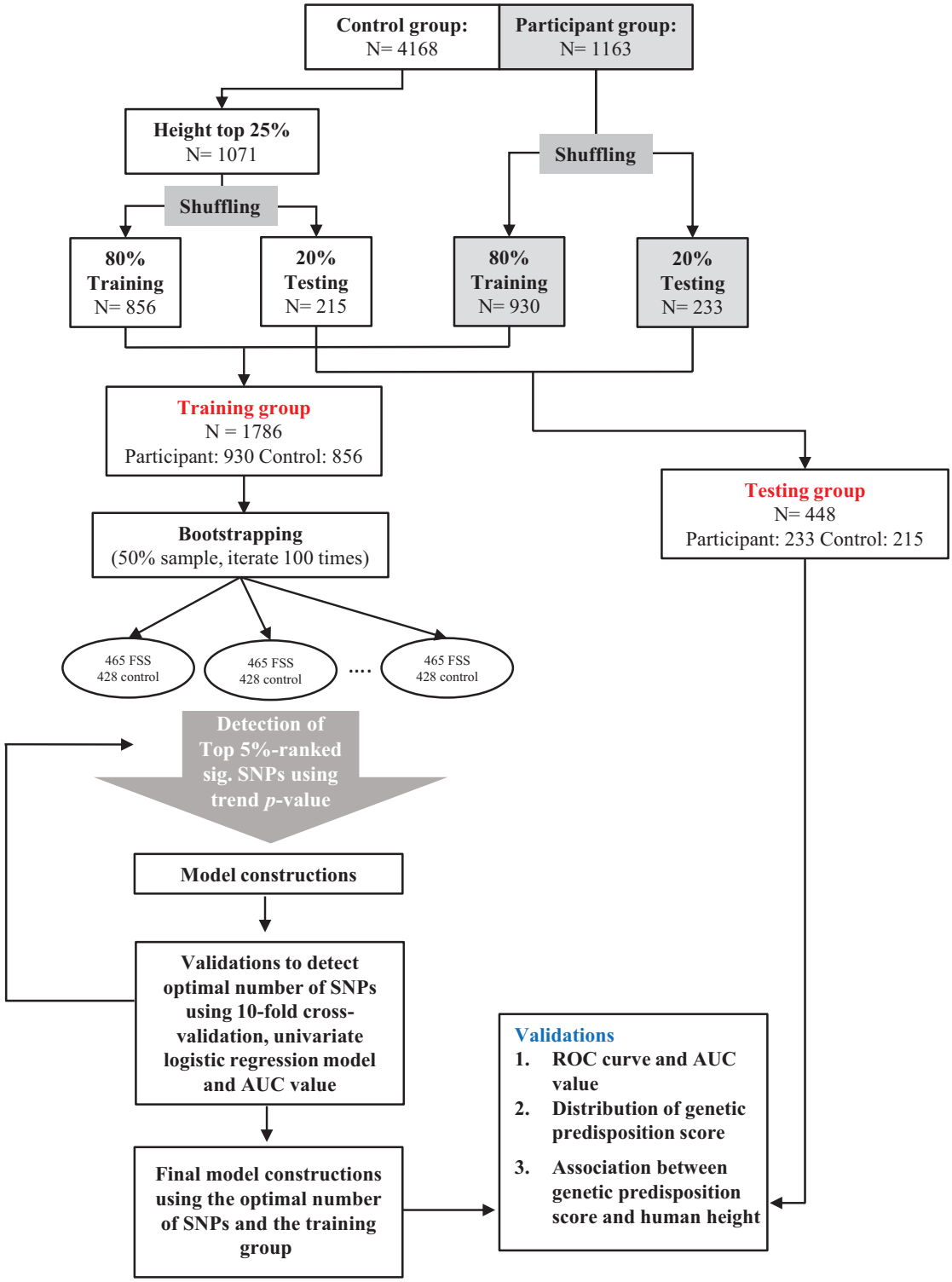

Figure 1. Flow diagram showing the analysis for this study. Abbreviations: AUC, area under the curve; FSS, familial short stature; N, number; ROC, receiver operating characteristic; SNP, single nucleotide polymorphism.

group from our cohorts with type 2 diabetes, the GWAS data of each patient with type 2 diabetes was genotyped using the Axiom genome-wide TWB array plate, the Affymetrix genome-wide human SNP array 6.0, and the Illumina HumanHap550-Duo BeadChip according to the manufacturer's procedure.

Because GWAS data were from different genotyping platforms, genotype imputations were performed in both participants with FSS and control groups according to a 2-step genotype imputation approach. We used SHAPEIT2 to pre-phase the study genotypes into full haplotypes (27). We then performed imputation

using IMPUTE2 and the Phase I 1000 Genomes Project reference panel (June 2011 interim release) consisting of 1094 phased individuals from multiple ancestry groups (the 1000 Genomes Project Consortium, 2010) (28). Finally, we used the GTOOL software (http://www.well.ox.ac.uk/~cfreeman/software/gwas/ gtool.html) to homogenize strand annotation by merging the imputed results obtained from each set of genotyped data.

Genotype and imputed genotype data were quality controlled, and genetic variants were excluded from further analysis if (1) (a) only 1 allele appeared in participants and/or control groups (2); (b) the total call rate was less than 95% for both participants and control groups (3); (c) the minor allele frequency was less than 0.5% in the control groups in the Han Chinese population (4); and (d) genetic variants significantly departed from Hardy-Weinberg equilibrium proportions ($P < 0.01$).

Genetic predisposition score calculation

The genetic predisposition score (also known as polygenic risk score or genetic risk score) is calculated by multiplying each beta coefficient (log odds ratio [OR]) value by the number of the corresponding risk allele under the additive model for each individual and then summing the products for the risk alleles identified from the multiple susceptible genetic variants (29). In this study, the genetic predisposition score was calculated based on the 10 genetic variants (SNPs). Each genetic variant was given a weightage based on the average effect size (beta coefficient) for the FSS obtained from our study (Table 1). The genetic predisposition score was calculated by multiplying each beta coefficient by the number of corresponding risk alleles (risk allele homozygote [the risk genotype is coded as "2"], risk allele heterozygote [the risk genotype is coded as "1"], and nonrisk allele homozygote [the nonrisk genotype is coded as "0"] according to the additive inheritance model) and then summing the products from these 10 genetic variants weighted by their estimated effect sizes (log OR).

Statistical analysis

All the genotyped and imputed GWAS results of participants with FSS and their control groups were used for association studies using a regression framework implemented in PLINK under the additive inherited genetic model (30). The difference in allelic frequency in the additive model between the participants and control groups was measured by odds ratios (ORs) with 95% confidence intervals (CIs) using logistical regression models (Tables 1–2 and Supplementary Tables 1–6 and

Table 1. Ten Novel Genetic Variants Associated With FSS Risk

Genetic variant (rs ID)	Gene	Chr	Position	Risk allele	Training Group (Participant: 930 and Control: 856)			Testing Group (Participant: 233 and Control: 215)			Total Groups (Participant: 1163 and Control: 1071)		
					OR	95% CI	*P* Value	OR	95% CI	*P* Value	OR	95% CI	*P* Value
rs202128628		2	91971930	T	9.89	(5.43- 18)	6.79E-14	8.70	(3.03- 25.01)	5.88E-05	9.59	(5.7 - 16.14)	1.80E-17
rs116988614	*COL6A5*	3	130092364	G	16.24	(11.4- 23.12)	6.62E-54	12.64	(7.06- 22.66)	1.51E-17	15.32	(11.33 - 20.73)	3.52E-70
rs2375843	*LOC105374144*	3	145352404	C	3.87	(3.33- 4.55)	1.40E-70	4.62	(3.36- 6.34)	2.60E-21	4.00	(3.45 - 4.55)	3.95E-90
rs525537		3	165355602	G	5.63	(4.55- 7.14)	4.01E-61	5.23	(3.53- 7.75)	1.37E-16	5.56	(4.55 - 6.67)	5.40E-76
rs367599822	*UGT2B17*	4	69412874	A	4.12	(4.84- 3.51)	4.69E-67	4.44	(3.21- 6.15)	2.74E-19	4.18	(3.62 - 4.82)	1.36E-84
rs7659854	*IQCM*	4	150692140	C	5.71	(4.93- 6.61)	2.42E-120	5.37	(4.04- 7.13)	4.73E-31	5.64	(4.95 - 6.42)	1.44E-149
rs13183322		5	109237379	C	1.93	(1.65- 2.25)	7.01E-17	1.77	(1.31- 2.4)	2.25E-04	1.90	(1.65 - 2.18)	7.76E-20
rs117002249		5	145793167	T	10.21	(5.56- 20)	4.53E-13	6.12	(2.32- 16.16)	2.50E-04	9.09	(5.26 - 14.29)	3.37E-16
rs7033295		9	2407693	G	4.94	(4- 6.25)	2.61E-43	4.53	(2.94- 6.99)	7.92E-12	4.76	(4 - 5.88)	1.42E-53
rs199690933	*PGM5P2*	9	69132306	T	5.04	(3.36- 7.57)	5.05E-15	5.55	(2.27- 13.55)	1.71E-04	5.13	(3.55 - 7.41)	3.88E-18

P value was expressed in exponential notation (The E is standard scientific notation for power of 10; for example: 6.79E-14 means 6.79×10^{-14}).
OR calculation was conducted according to the defined risk alleles.Abbreviations: Chr, chromosome; CI, confidence interval; FSS, familial short stature; OR, odds ratio.

Table 2. Nine Human Height-Related Genetic Variants Associated With FSS Risk

Genetic Variant (rs ID)	Gene	Chr	Position	Risk Allele	Reference	PMID Number	Population	Training Group (Participant 930 and Control: 856)			Testing Group (Participant 233 and control: 215)			Total groups (Participant 1,163 and control: 1,071)		
								OR	95% CI	*P* Value	OR	95% CI	*p* value	OR	95% CI	*p* value
rs2421992	*DNM3*	1	172241251	C	Wood AR et al, 2014	25282103	European	4.35	(3.85-5.00)	5.72E-93	5.00	(3.7 - 6.67)	1.37E-27	4.55	(4.00 - 5.00)	8.78E-119
rs4974480	*ANAPC13*	3	134178562	A	Wood AR et al, 2014	25282103	European	1.33	(1.14-1.54)	3.05E-04	1.55	(1.15 - 2.10)	4.33E-03	1.37	(1.20 - 1.57)	6.21E-06
rs13131350	*LCORL*	4	17877487	G	He M et al, 2015	25429064	European, East Asian	1.30	(1.12-1.49)	3.92E-04	1.40	(1.06 - 1.85)	1.83E-02	1.32	(1.16 - 1.50)	2.31E-05
rs7763064	*GPR126*	6	142797289	A	Lango Allen H et al, 2010	20881960	European	1.23	(1.07-1.41)	3.26E-03	1.19	(0.91 - 1.55)	1.99E-01	1.22	(1.08 - 1.38)	1.36E-03
rs10858250	*QSOX2*	9	139119215	A	He M et al, 2015	25429064	European, East Asian	1.23	(1.05-1.45)	8.53E-03	1.37	(1.00 - 1.85)	5.08E-02	1.27	(1.10 - 1.47)	1.21E-03
rs11170631	*ATF7-ATP5G2*	12	54041192	T	Okada Y et al, 2010	20189936	Japanese	1.35	(1.18-1.56)	1.57E-05	1.43	(1.09 - 1.89)	1.18E-02	1.37	(1.20 - 1.56)	6.08E-07
rs258324	*CDK10*	16	89754255	G	He M et al, 2015	25429064	East Asian	1.19	(1.03-1.39)	1.61E-02	1.32	(0.99 - 1.79)	6.14E-02	1.22	(1.08 - 1.39)	2.80E-03
rs8094261	*CABLES1*	18	20746728	G	Kim JJ et al, 2010	19893584	Korean	1.38	(1.16-1.64)	2.57E-04	1.33	(0.94 - 1.88)	1.05E-01	1.37	(1.17 - 1.6)	6.46E-05
rs4911494	*UQCC1*	20	33971914	T	Soranzo N et al, 2009	19343178	European	1.33	(1.15-1.54)	1.26E-04	1.22	(0.89 - 1.67)	2.08E-01	1.32	(1.15 - 1.49)	6.12E-05

OR calculation was conducted according to the defined risk alleles. Deviation from the additive model was tested. A *P* value for the additive test < 0.05 in the training group was considered significant.
Abbreviations: Chr, chromosome; CI, confidence interval; FSS, familial short stature; ID, identifier; PMID, PubMed identifier; OR, odds ratio.

8–9) (26). All data management and statistical analyses were performed using PLINK and SAS software (version 9.4; SAS Institute, Cary, NC, USA).

For haplotype block analysis, the Lewontin D′ and R^2 values were used to evaluate the intermarker coefficient of linkage disequilibrium (LD) in both participants with FSS and control groups (31). The CI for LD was estimated using a resampling procedure and was used to construct the haplotype blocks (Supplementary Fig. S3) (26, 32, 33).

The risk prediction model predicts the health outcome by using several predictor variables based on the observed patient's characteristics (34). Risk prediction was evaluated by the area under the receiver operating characteristic (ROC) curves (AUCs). The AUC ranged from 0.5 (total lack of discrimination) to 1.0 (perfect discrimination). AUCs were calculated for the predicted risks of 10 novel, 9 reported, and combined SNPs, respectively (Figs. 2a and 2b).

For the linear human height curve model, participants with the genetic predisposition score calculated from the 10 novel SNPs (Fig. 3a) and 9 human height-related SNPs (Fig. 3b) were used as continuous variables in a linear regression with human height (cm) as the dependent variable, respectively.

Results

Bootstrap ranking identifies 10 novel and 9 human height GWAS-reported SNPs robustly associated with FSS

The flowchart of enrollment of participants with FSS is shown (Supplementary Fig. S1) (26). Participants for controls were recruited when their body heights

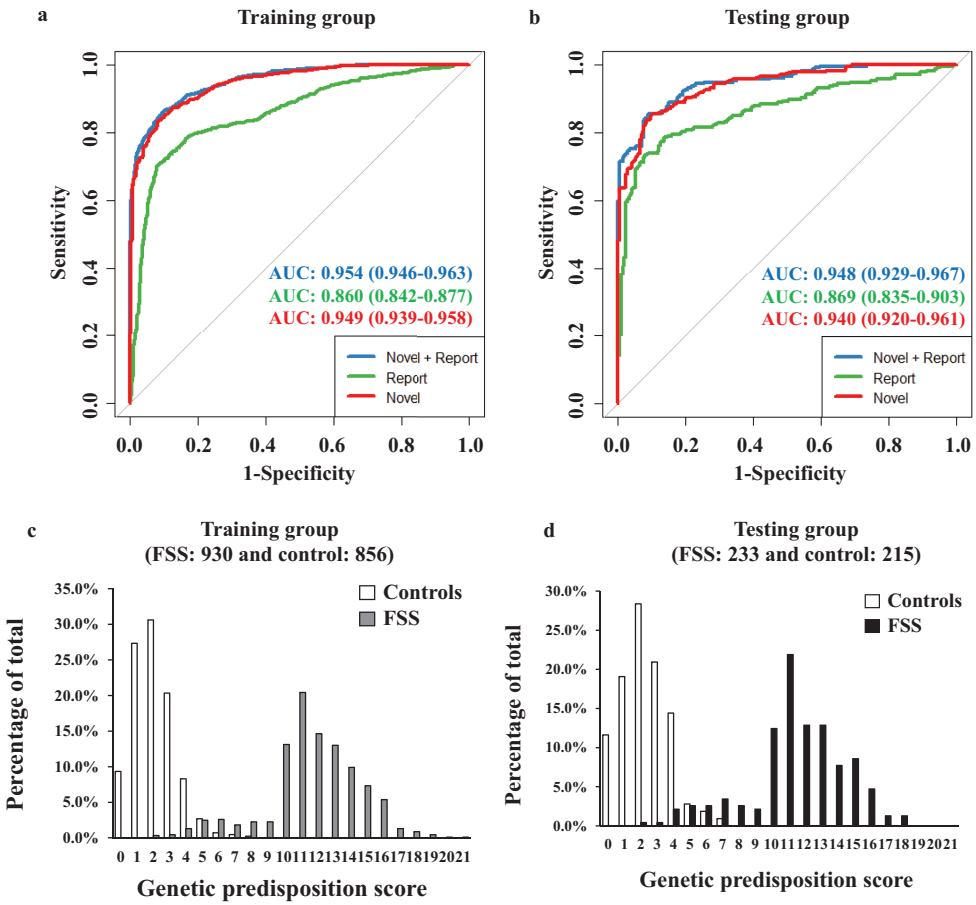

Figure 2. Receiver operating characteristic (ROC) curves, area under the curve (AUC) values, and distribution of the genetic predisposition score for familial short stature (FSS) among training and testing groups, respectively. (**a**) ROC curves and AUC values for 10 novel single nucleotide polymorphisms (SNPs; Novel), 9 reported SNPs (Report), and 10 novel and 9 reported SNPs (Novel + Report) in the training group. The 10 novel SNPs showed the AUC value (AUC = 0.949); the 9 reported SNPs showed the AUC value (AUC = 0.955); the 10 novel + 9 reported SNPs showed the AUC value (AUC = 0.954). (**b**) ROC curves and AUC values for 10 novel SNPs (Novel), 9 reported SNPs (Report), and 10 novel + 9 reported SNPs (Novel + Report) in the testing group. The 10 novel SNPs showed the AUC value (AUC = 0.940); the 9 reported SNPs showed the AUC value (AUC = 0.869); the 10 novel and 9 reported SNPs showed the AUC value (AUC = 0.948). (**c**) The distribution of the genetic predisposition score from 10 novel SNPs between FSS and control groups in the training group (FSS: gray square; Controls: white square). (**d**) Distribution of the genetic predisposition score from 10 novel SNPs between FSS and control groups in the testing group (FSS: black square; Controls: white square).

Figure 3. Association between genetic predisposition score (GRS) and human height for male and female participants. Human height (cm) values are shown with respect to genetic predisposition score values. The mean ± 95% confidence interval was plotted. *P value < 0.05. (**a**) Participants with their genetic predisposition score of 10 novel single nucleotide polymorphisms (SNPs) and human height information were recruited and divided into male and female participants (male participants*, N = 2146; female participants*, N = 2022). (**b**) Participants with their genetic predisposition score of 9 human height-related SNPs and human height information were recruited and divided into male and female participants (Male participants*, N = 2146; female participants*, N = 2022).

exceeded that of the top 75th percentile of the general population in Taiwan. All the participants and control groups were of Han Chinese ancestry and were located in the East Asian population using principal component analysis (Supplementary Fig. S2) (26).

As shown in Fig. 1, participants with FSS and their control groups were randomly shuffled and assigned into the training (80% of the total population) and testing (20% of the total population) groups. For the training group, 930 participants and 856 control participants served as the discovery stage for subsequent model construction and validation to obtain an optimal number of SNPs using AUC values. Bootstrapping 50% subsampling and GWAS analyses iterated 100 times were performed (Fig. 1) (23, 24). The top 5%-ranked significant SNPs were obtained using the Cochran-Armitage trend P value. In the SNP list, there were 155 SNPs with P values < 1.00^{-10} under the Cochran-Armitage trend model (Supplementary Table S1) (26). For the testing group, 233 participants and 215 control participants served as the examination stage for validation including the ROC curve and AUC values, distribution of genetic predisposition scores, and association between genetic predisposition scores and human height (Fig. 1).

To obtain the optimal number of SNPs for the risk prediction model in the testing group, 10-fold cross-validation, univariate logistic regression model, and AUC value were obtained for the training group (Fig. 1; Supplementary Fig. S5) (26). These resulted in 10 novel SNPs (Table 1). The pair-wise LD for the 10 novel SNPs was also considered to prevent a miscalculation of the cumulative effect of these identified SNPs (Supplementary Fig. S3) (26, 31–33). SNPs with strong LD ($D' > 0.8$) were excluded. These results suggest that these 10 novel SNPs were independent from each other, and thus were used to obtain AUC values, distribution of genetic predisposition scores, and association between genetic predisposition scores and human height (Figs. 2 and 3). In the training group, the highest AUC value for the 10 novel SNPs was observed (Fig. 2a; AUC = 0.949). In the testing group, the highest AUC value for 10 novel SNPs was observed (Fig. 2b; AUC = 0.940). These 10 novel SNPs within the 5 closest genes were rs202128628 and rs116988614 in *COL6A5*; rs2375843 in *LOC105374144* (a non-coding ribonucleic acid gene); rs525537 and rs367599822 in *UGT2B17*; rs7659854 in *IQCM*; and rs13183322, rs117002249, rs7033295, and rs199690933 in *PGM5P2* (Table 1).

Furthermore, genetic predisposition to human height has been reported (4–14). To investigate the associations between these known GWAS human height-related SNPs and FSS risk, we then evaluated their associations using the P value under the Cochran-Armitage trend model in our training group. There were 678 human height-related genetic variants investigated in this study (Supplementary Table S2) (26). There were 114 SNPs with a P value for the additive model of < 0.05 in the training group (Supplementary Table S2) (26). After validation using MALDI-TOF mass spectrometry-based SNP genotyping and LD analysis (not shown), the

resultant re-selected 9 SNPs are summarized in Table 2. After replication in the testing group, these 9 SNPs were associated with FSS risk with a *P* value for the additive model of < 0.05 in the total groups. These 9 genetic variants within the 9 closest genes were rs2421992 in *DNM3*, rs4974480 in *ANAPC13*, rs13131350 in *LCORL*, rs7763064 in *GPR126*, rs10858250 in *QSOX2*, rs11170631 in *ATF7-ATP5G2*, rs258324 in *CDK10*, rs8094261 in *CABLES1*, and rs4911494 in *UQCC1*.

ROC curve and AUC value in risk prediction model for FSS

Figures 2a and 2b show the ROC curves for risk prediction for FSS based on the 10 novel, 9 reported, and combined SNPs in the training and testing groups, respectively. In the training group, the AUC was 0.949 (95% CI, 0.939-0.958) for prediction based on the 10 novel SNPs; 0.860 (0.842-0.877) for 9 reported SNPs; and 0.954 (0.946-0.936) for the combined 10 novel and 9 reported SNPs (Fig. 2a).

To ensure robust analysis, the testing group was also applied for final validation and evaluation of the performance of risk prediction models for FSS. In the testing group, the AUC was 0.940 (95% CI, 0.920-0.961) for prediction based on the 10 novel SNPs; 0.869 (0.835-0.903) for 9 reported SNPs; and 0.948 (0.929-0.967) for the combined 10 novel and 9 reported SNPs (Fig. 2b). There was no significant increase in the AUC with the combined 10 novel and 9 reported SNPs when compared with that with the 10 novel SNPs in the training and testing groups, respectively (Figs. 2a and 2b). These results suggest that the 10 novel SNPs are important for FSS risk prediction.

Distribution of genetic predisposition score

Table 1 shows the OR (beta coefficient) associated with the risk allele for each of the 10 novel SNPs in a logistic regression model. In this study, the genetic predisposition score was calculated based on summing of the risk alleles from these 10 novel SNPs by multiplying each beta coefficient (log OR) by the number of corresponding risk allele under the additive model. The frequency distribution of individuals carrying the calculated genetic predisposition score between groups with FSS and control groups is shown in the training and testing groups, respectively (Figs. 2c and 2d). There were significant differences in the distributions of genetic predisposition scores in both the training and testing groups. In the training group, 88.8% had their genetic predisposition score ≥ 9 from FSS, whereas 0.0% had their genetic predisposition score ≥ 9 from the control groups. Similarly, in the testing group, 85.8% had their genetic predisposition score ≥ 9 from FSS, whereas 0.0% had their genetic predisposition score ≥ 9 from the control groups.

The distributions of genetic predisposition score for FSS and control groups were also divided into quartiles (quartile 1-quartile 4; Table 3). Individuals in quartile 1 served as a reference. There was a continuous increasing trend in FSS risk with cumulative genetic predisposition score ($P < 0.0001$; Cochran-Armitage trend test). Compared with individuals in quartile 1, those in quartiles 2 and 3 showed association with increased FSS risk in a dose-dependent manner (quartile 2: OR, 3.02 [2.16-4.21]; quartile 3: OR, 23.56 [16.93-32.79]). There were no individuals with quartile 4 in the control groups (0.0%); however, there were 543 individuals (64.7%) with quartile 4 in the FSS group. These results suggest that there was a cumulative effect of these 10 novel SNPs on FSS risk.

Association between genetic predisposition score and human height

The association between genetic predisposition score and human height was also investigated to explore their linear regression when stratified by gender (male: N = 2146; female: N = 2022; Fig. 3a and 3b). Figure 3a

Table 3. Cumulative Effect of the 10 Novel Genetic Variants Associated With FSS Risk

	FSS (%)	Controls (%)			
	N = 1163	N = 1071			
Quartile of Genetic Score	N (%)	N (%)	OR	95% CI	*P* Value
Quartile 1 (score ≤ 7.0)	57 (4.9%)	496 (46.3%)	Ref	Ref	Ref
Quartile 2 (7.0 < score ≤ 8.7)	146 (12.6%)	421 (39.3%)	3.02	2.16-4.21	*< 0.0001*
Quartile 3 (8.7 < score ≤ 14.4)	417 (35.9%)	154 (14.4%)	23.56	16.93-32.79	*< 0.0001*
Quartile 4 (score > 14.4)	543 (64.7%)	0 (0%)	> 999	0.001-999	0.934
Cochran-Armitage trend test					*< 0.0001*

The cumulative effect was investigated in the combination of the training and testing groups. The FSS 10 novel genetic variants and their respective risk genotypes were shown in Table 1. Quartile of genetic score was calculated using the cumulation of the 10 genetic variants described in materials and methods. Abbreviations: CI, confidence interval; FSS, familial short stature; N, number; OR, odds ratio; Ref, reference.

shows plots of the genetic predisposition score of males (N = 2146) calculated from these 10 novel genetic variants and the corresponding human height information (cm). The regression line indicated that a 1-unit difference in genetic predisposition score was associated with a reduction of 0.29 cm in height (slope = –0.29; $P = 0.00265$; human height = 169 cm – 0.29 cm × genetic predisposition score) (Fig. 3a). For females (N = 2022), the regression line indicated that a 1-unit difference in genetic predisposition score was associated with a reduction of 0.244 cm in human height (slope = –0.244; $P = 0.009331$; human height = 157 cm – 0.244 cm × genetic predisposition score) (Fig. 3a).

Figure 3b shows plots of the genetic predisposition score of males (N = 2146) from 9 human height-related SNPs and the corresponding human height information (cm). The regression line indicated that a 1-unit difference in genetic predisposition score was associated with a reduction of 0.224 cm in height (slope = –0.224; $P < 0.0001$; human height = 169 cm – 0.224 cm × genetic predisposition score) (Fig. 3b). For females (N = 2022), the regression line indicated that a 1-unit difference in genetic predisposition score was associated with a reduction of 0.0826 cm in height (slope = –0.0826; $P = 0.009572$; human height = 156 cm – 0.0826 cm × genetic predisposition score) (Fig. 3b). These results suggest that the 10 novel and 9 reported genetic SNPs were associated with height reduction.

Discussion

Osteoclasts and chondrocytes play important roles in growth plate as well as human height regulation. In the growth plate, osteoclast activity regulates the mineralization of highly differentiated hypertrophic chondrocytes (18). Chondrocytes also play important roles in bone growth and homeostasis of the growth plate in bone biology (19). In this study, we identified 10 novel and 9 reported GWAS human height-related SNPs associated with FSS risk. These 10 novel SNPs are a genetic biomarker for FSS risk prediction and are associated with a height reduction regression tendency.

In our previous study, there were 978 participants with FSS and 1129 control participants with their height above the top 75th percentile (1). There were 1033 SNPs in 14 human height GWAS used to evaluate the difference between participants with FSS and control participants (1). As shown, there were 34 SNPs associated with FSS (call rate > 95%, $P > 0.05$ for Hardy-Weinberg equilibrium, and $P < 5.00E\text{-}05$ (0.05/1033) for the additive model). The LD among these 34 SNPs was determined and the resultant re-selected 13 SNPs were then used for polygenic risk score calculation. The design of the current study included 930 participants with FSS and 856 control participants with their height above the top 75th percentile. In this study, 678 human height-related SNPs were investigated (Supplementary Table S2) (26). There were 114 SNPs with a P value for the additive model of < 0.05 in the training group (Supplementary Table S2) (26). After validation using MALDI-TOF mass spectrometry-based SNP genotyping and LD analysis (not shown), the resultant re-selected 9 SNPs are shown. After replication in the testing group, these 9 SNPs were associated with FSS risk with a P value for the additive model < 0.05 in total groups. These 9 SNPs were then used for FSS risk prediction and height association. Therefore, owing to the differences in number of the human height GWAS-related SNPs, participant number, control number, and, selection for P value for the additive model used in this study, it may result in the elimination from the current paper of the 10 other Taiwanese genes associated with FSS listed in our previous study.

The 10 FSS novel SNPs were mapped to genes such as *COL6A5*, *LOC105374144*, *UGT2B17*, *IQCM*, and *PGM5P2*. The 10 novel SNPs were suitable for distinguishing between the FSS and control subgroups (non-FSS) (Supplementary Figs., 6–7 andSupplementary Table 3) (26). However, these SNPs were not suitable for distinguishing between the 97th percentile control and short groups including the third percentile control and 25th percentile control groups (Supplementary Table 5) (26). Among these genes, we identified genetic variants in *COL6A5* within at least 2 SNPs (rs116988614 and rs117620786). *COL6A5* encodes a member of the supramolecular assembly of collagen VI (ColVI) of the collagen family (35). ColVI is encoded by 6 different genes, *COL6A1*, *COL6A2*, *COL6A3*, *COL6A4*, *COL6A5*, and *COL6A6*. ColVI is involved in the formation of the extracellular matrix of articular cartilage and fetal bone. In the fetal stage, ColVI is located in discrete fibrils in the fetal bone during development (36). In the adult stage, ColVI is mainly located in the pericellular matrix of the cartilage to maintain the integrity of chondrocytes (37). In addition, soluble ColVI has been used as an important stimulant for the expansion and proliferation of chondrocytes (38). Alternative expression or mutations of genes encoding ColVI are associated with changes in bone mineral density, atopic dermatitis, familial neuropathic chronic itch, and musculoskeletal abnormalities such as Bethlem myopathy, Ullrich congenital muscular dystrophy, osteopenia, and other bone and cartilage disorders (39–41).

We also observed that the genetic variant rs367599822, located in *UGT2B17,* was associated with FSS risk. *UGT2B17* encodes the uridine 5'-diphosphoglucuronosyltransferase [UDP]-2B17 protein (42), which is involved in testosterone metabolism and assists in transferring UDP-glucuronic acid to testosterone to increase its renal excretion (43). *UGT2B17* is also associated with body mass index, fat mass, male insulin sensitivity, bone mineral density, osteoporosis, and prostate cancer (44–48). Individuals with homozygous deletions of *UGT2B17* had significantly higher concentrations of total serum testosterone and estradiol than those with 1 or 2 copies of this gene (47). Both sex hormones are required for cancellous bone mass and integrity (49–53). In early puberty, both sex hormones stimulate fast pubertal growth in human height along with growth hormone (GH) and insulin-like growth factor (IGF)-1 (54). Testosterone increases the width of the epiphyseal growth plate by promoting osteoblast proliferation and differentiation and inhibiting osteoclast activity and apoptosis (50, 51, 55). Estradiol produced from testosterone promotes osteoclast apoptosis and inhibits osteoclast activity (52, 53). At the end of puberty, high levels of estradiol promote the fusion of the epiphyseal growth plate by stimulating chondrocyte maturation and inhibiting its proliferation (56). Therefore, *UGT2B17* may affect human height as well as FSS by modulating serum levels of sex hormones and regulating bone and chondrocyte metabolism. Biological studies warrant further investigations in the role of *UGT2B17* in the cell proliferations and differentiations of chondrocyte/osteocyte progenitor cells.

Genetic variant rs7659854 in *IQCM* (also known as *LOC285423*), encoding IQ motif containing M, was associated with FSS risk. However, its biological function remains to be elucidated. Recently, the genetic variants located with this gene were associated with hypothyroidism (57). Hypothyroidism is an endocrine disorder, in which the thyroid gland does not produce sufficient thyroid hormone. Thyroid hormone, as well as GH, IGF-1, and androgens, can stimulate chondrogenesis and also regulate proliferation and/or differentiation of multiple cell types in bone, including chondrocytes, osteoblasts, and osteoclasts (58). Therefore, hypothyroidism is also associated with short stature (59, 60). Furthermore, we identified a genetic variant rs199690933 in *PGM5P2* to be associated with FSS. *PGM5P2* encodes phosphoglucomutase 5 pseudogene 2, which is involved in pathological processes in the fibroblast-like synoviocytes from patients with rheumatoid arthritis (61). However, the roles of *PGM5P2* in adult height and FSS remain unclear and further functional characterization is required.

The 9 human height-related genetic variants were associated with FSS and were mapped to the genes *DNM3*, *ANAPC13*, *LCORL*, *GPR126*, *QSOX2*, *ATF7-ATP5G2*, *CDK10*, *CABLES1,* and *UQCC1*. The 7 of 9 human height-related SNPs were suitable for distinguishing between the FSS and taller groups including the 97th percentile, 75th percentile, and 50th percentile control groups (Supplementary Figs, 6–7 and Supplementary Table 4) (26). However, these 9 SNPs might not be suitable for distinguishing between the FSS and shorter groups including the 25th percentile and 3rd percentile control groups (Supplementary Table 4) (26). The 5 of 9 human height-related SNPs might be suitable for distinguishing between the 97th percentile control and shorter groups including the FSS, 3rd percentile control groups, and 25th percentile control groups (Supplementary Table 6) (26). Network cluster analysis revealed functions of these genes, which are mainly related to cancer, organismal injury and abnormalities, and reproductive system disease (Supplementary Fig. S4) (26). *DNM3* encodes a member of the family of guanosine triphosphate-binding proteins that associate with microtubules and are involved in vesicular transport and megakaryocyte development (62, 63). Genetic variants in *DNM3* are associated with human height (4, 10, 64). *ANAPC13* encodes a component of the anaphase-promoting complex, a large ubiquitin-protein ligase that controls cell cycle progression by regulating the degradation of cell cycle regulators such as cyclin B (65, 66). Genetic variants in *ANAPC13* are associated with human height (5, 7). Genetic variant rs13131350 within *LCORL* was associated with FSS in our study (1) and was also reported in a meta-analysis study of GWAS of adult height in East Asians (64). *GPR126* encodes a G-protein–coupled receptor, genetic variations that are associated with human height (4, 10, 14, 64). Similarly, genetic variations in *QSOX2,* which encodes a member of the sulfhydryl oxidase/quiescin-6 family (67) are associated with human height (4, 9, 64, 68). *ATF7* encodes activating transcription factor 7 and is involved in cell cycle regulation and proliferation (69); genetic variants of *ATF7* are associated with human height (9, 64, 70). SNPs *in ATP5G2*, which encodes a mitochondrial ATP synthase (71), are also associated with human height (9, 64). We detected one FSS-associated SNP (rs258324) in *CDK10* (1), which was also reported in a human height GWAS (64). Genetic variations rs4308051 and rs8094261 (1) in *CABLES1* are associated with FSS in Han Chinese people in Taiwan and have also been reported in human height GWAS (1, 4, 8, 13, 64). *UQCC1* encodes ubiquinol-cytochrome c reductase complex assembly factor 1, a transmembrane

protein involved in fibroblast growth factor-regulated growth control, bone growth, and development (72). SNPs in *UQCC1* are associated with human height (6, 7, 10, 14, 64, 73). Therefore, FSS may partially overlap with human height-related genetic variants, which are related to height-reducing effects.

An initial GWAS was also performed between the 97th percentile and 25th percentile control groups (Supplementary Tables 7–8) (26). The top 53 significant SNPs were found between the 97th percentile control and 25th percentile control groups ($P < 1.00E-5$). There were no overlapping SNPs between the top 155 FSS-related SNPs ($P < 1.00E-10$) and these top 53 SNPs (Supplementary Tables 1 and 8) (26). These results suggested that there are distinct different genetic profiles between the FSS and 97th percentile control groups.

Plachy et al (74) reported that there are 14 genes with missense mutations that have been identified in 33 participants with severe FSS using whole-exome sequencing. As Plachy et al reported, the authors chose 33 participants with severe FSS (their height –2.5 SD or less in both the patients and the shorter parent), which was suggested as a monogenic condition (74). Whole-exome sequencing analysis was then performed for the participants with severe FSS (74). In addition, among these 33 participants with severe FSS, 21 (64%) of them were born small for gestational age. And among these 33 participants, 23 (70%) of them were classified with GH deficiency. In our study, we recruited participants with FSS of Han Chinese ancestry. The selection criteria for FSS was (1) (a) height less than the third percentile (Supplementary Fig. 7) (2, 26) (b) the parents' (father and/or mother) height less than the third percentile (3), (c) bone age appropriate for chronologic age (4), (d) normal onset of puberty (5), (e) normal annual growth rate, and (6) (f) normal results of clinical biochemistry examination. Excluded individuals were those with all other abnormal morphology and karyotyping results, abnormal bone age or puberty stage, or abnormal serum or plasma levels of clinical biochemistry examinations for the GH-IGF1 axis, thyroid function, or precocious puberty (Supplementary Fig. S1) (26). Therefore, the FSS participant characteristics may account for the differences between these 2 studies. Furthermore, we found that genetic variants in 9 of these 14 genes were associated with FSS risk between our 1163 participants with FSS and 1071 control participants (the 75th height percentile) (Supplementary Table 9 and Supplementary Fig. 8) (26). These 9 genes include *COL11A1*, *FLNB*, *FGFR3*, *TRHR*, *COL2A1*, *HMGA2*, *ACAN*, *IGF1R*, and *NF1*. These results suggested that, in addition to mutations in these genes, there might also be a combined effect of multiple genetic variants (polygenic effect) for developing the FSS risk.

The main limitations of our study are the small number of individuals with FSS since these individuals' body heights are below the third percentile of the population. We may have small effect sizes. Nevertheless, our study is the first comprehensive investigation of FSS genetic profile. Ten novel and 9 reported GWAS human height-related SNPs were revealed to be associated with FSS risk. These 10 novel genetic SNPs exhibited cumulative effect as genetic predisposition score and facilitated FSS risk prediction. A height reduction regression tendency in the general population was also observed between cumulative genetic predisposition score and human height regardless of gender. Our work found the FSS genetic characteristics and their bone metabolic association with the height-reduction effect.

Acknowledgements

We thank the National Center for Genome Medicine of the National Core Facility Program for Biotechnology, Ministry of Science and Technology, for technical and bioinformatics support. We also thank Drs. Kuan-Teh Jeang and Willy W.L. Hong for technical help and suggestions.

Financial Support: This study was supported by grants from the China Medical University (CMU108-MF-32, CMU108-S-15, and CMU108-S-17), the China Medical University Hospital (DMR-109–145, DMR-109–188, and DMR-109–192), and the Ministry of Science and Technology, Taiwan (MOST 105-2314-B-039 -037 -MY3, MOST 106-2320-B-039 -017 -MY3, and MOST 108-2314-B-039-044-MY3). We are grateful to Health Data Science Center, China Medical University Hospital for providing administrative, technical, and funding support.

Additional Information

Correspondence and Reprint Requests: Fuu-Jen Tsai, MD, PhD, Genetic Center, Department of Medical Research, China Medical University Hospital, Taichung 40447, Taiwan. E-mail: d0704@mail.cmuh.org.tw.

Disclosure Summary: The authors have no conflicts of interest to disclose.

Ying-Ju Lin and Chi-Fung Cheng contributed equally to this work.

Data Availability:Restrictions apply to the availability of data generated or analyzed during this study to preserve patient confidentiality or because they were used under license. The corresponding author will on request detail the restrictions and any conditions under which access to some data may be provided.

References

1. Lin YJ, Liao WL, Wang CH, et al. Association of human height-related genetic variants with familial short stature in Han Chinese in Taiwan. *Sci Rep*. 2017;**7**(1):6372.
2. Marouli E, Graff M, Medina-Gomez C, et al. Rare and low-frequency coding variants alter human adult height. *Nature*. 2017;**542**(7640):186–190.
3. Zoledziewska M, Sidore C, Chiang CWK, et al. Height-reducing variants and selection for short stature in Sardinia. *Nat Genet*. 2015;**47**(11):1352–1356.
4. Lango Allen H, Estrada K, Lettre G, et al. Hundreds of variants clustered in genomic loci and biological pathways affect human height. *Nature*. 2010;**467**(7317):832–838.
5. Wood AR, Esko T, Yang J, et al. Defining the role of common variation in the genomic and biological architecture of adult human height. *Nat Genet*. 2014;**46**(11):1173–1186.
6. Lettre G, Jackson AU, Gieger C, et al. Identification of ten loci associated with height highlights new biological pathways in human growth. *Nat Genet*. 2008;**40**(5):584–591.
7. Weedon MN, Lango H, Lindgren CM, et al. Genome-wide association analysis identifies 20 loci that influence adult height. *Nat Genet*. 2008;**40**(5):575–583.
8. Kim JJ, Lee HI, Park T, et al. Identification of 15 loci influencing height in a Korean population. *J Hum Genet*. 2010;**55**(1):27–31.
9. Okada Y, Kamatani Y, Takahashi A, et al. A genome-wide association study in 19 633 Japanese subjects identified LHX3-QSOX2 and IGF1 as adult height loci. *Hum Mol Genet*. 2010;**19**(11):2303–2312.
10. Gudbjartsson DF, Walters GB, Thorleifsson G, et al. Many sequence variants affecting diversity of adult human height. *Nat Genet*. 2008;**40**(5):609–615.
11. Yang J, Ferreira T, Morris AP, et al. Conditional and joint multiple-SNP analysis of GWAS summary statistics identifies additional variants influencing complex traits. *Nat Genet*. 2012;**44**(4):369–375, S361-363.
12. Cho YS, Go MJ, Kim YJ, et al. A large-scale genome-wide association study of Asian populations uncovers genetic factors influencing eight quantitative traits. *Nat Genet*. 2009;**41**(5):527–534.
13. Chan Y, Salem RM, Hsu YH, et al. Genome-wide analysis of body proportion classifies height-associated variants by mechanism of action and implicates genes important for skeletal development. *Am J Hum Genet*. 2015;**96**(5):695–708.
14. Soranzo N, Rivadeneira F, Chinappen-Horsley U, et al. Meta-analysis of genome-wide scans for human adult stature identifies novel loci and associations with measures of skeletal frame size. *Plos Genet*. 2009;**5**(4):e1000445.
15. Christesen HT, Pedersen BT, Pournara E, Petit IO, Júlíusson PB. Short stature: comparison of WHO and national growth standards/references for height. *Plos One*. 2016;**11**(6):e0157277.
16. Florencio-Silva R, Sasso GR, Sasso-Cerri E, Simões MJ, Cerri PS. Biology of bone tissue: structure, function, and factors that influence bone cells. *Biomed Res Int*. 2015;**2015**:421746.
17. Baek WY, Kim JE. Transcriptional regulation of bone formation. *Front Biosci (Schol Ed)*. 2011;**3**:126–135.
18. van der Eerden BC, Karperien M, Wit JM. Systemic and local regulation of the growth plate. *Endocr Rev*. 2003;**24**(6):782–801.
19. Aghajanian P, Mohan S. The art of building bone: emerging role of chondrocyte-to-osteoblast transdifferentiation in endochondral ossification. *Bone Res*. 2018;**6**:19.
20. Lindsay R, Feldkamp M, Harris D, Robertson J, Rallison M. Utah Growth Study: growth standards and the prevalence of growth hormone deficiency. *J Pediatr*. 1994;**125**(1):29–35.
21. Moore KC, Donaldson DL, Ideus PL, Gifford RA, Moore WV. Clinical diagnoses of children with extremely short stature and their response to growth hormone. *J Pediatr*. 1993;**122**(5 Pt 1):687–692.
22. Sisley S, Trujillo MV, Khoury J, Backeljauw P. Low incidence of pathology detection and high cost of screening in the evaluation of asymptomatic short children. *J Pediatr*. 2013;**163**(4):1045–1051.
23. Manor O, Segal E. Predicting disease risk using bootstrap ranking and classification algorithms. *Plos Comput Biol*. 2013;**9**(8):e1003200.
24. Eccles DA, Lea RA, Chambers GK. Bootstrap distillation: non-parametric internal validation of GWAS results by subgroup resampling. *bioRxiv*. 2017;**104497**.
25. World Medical A. World Medical Association Declaration of Helsinki: ethical principles for medical research involving human subjects. *JAMA*. 2013;**310**(20):2191–2194.
26. Lin YJ, Cheng CF, Wang CH, et al. Data from: Genetic architecture associated with familial short stature. *Dryad Digital Repository*. 2020; Deposited 4th January 2020. doi:10.5061/dryad.vhhmgqnpk
27. Delaneau O, Zagury JF, Marchini J. Improved whole-chromosome phasing for disease and population genetic studies. *Nat Methods*. 2013;**10**(1):5–6.
28. Howie BN, Donnelly P, Marchini J. A flexible and accurate genotype imputation method for the next generation of genome-wide association studies. *Plos Genet*. 2009;**5**(6):e1000529.
29. Cooke Bailey JN, Igo RP Jr. Genetic risk scores. *Curr Protoc Hum Genet*. 2016;**91**:1.29.1–1.29.9.
30. Purcell S, Neale B, Todd-Brown K, et al. PLINK: a tool set for whole-genome association and population-based linkage analyses. *Am J Hum Genet*. 2007;**81**(3):559–575.
31. Barrett JC, Fry B, Maller J, Daly MJ. Haploview: analysis and visualization of LD and haplotype maps. *Bioinformatics*. 2005;**21**(2):263–265.
32. Gabriel SB, Schaffner SF, Nguyen H, et al. The structure of haplotype blocks in the human genome. *Science*. 2002;**296**(5576):2225–2229.
33. Lin YJ, Wan L, Wu JY, et al. HLA-E gene polymorphism associated with susceptibility to Kawasaki disease and formation of coronary artery aneurysms. *Arthritis Rheum*. 2009;**60**(2):604–610.
34. Pavlou M, Ambler G, Seaman SR, et al. How to develop a more accurate risk prediction model when there are few events. *BMJ*. 2015;**351**:h3868.
35. Cescon M, Gattazzo F, Chen P, Bonaldo P. Collagen VI at a glance. *J Cell Sci*. 2015;**128**(19):3525–3531.
36. Keene DR, Sakai LY, Burgeson RE. Human bone contains type III collagen, type VI collagen, and fibrillin: type III collagen is present on specific fibers that may mediate attachment of tendons, ligaments, and periosteum to calcified bone cortex. *J Histochem Cytochem*. 1991;**39**(1):59–69.
37. Wu JJ, Eyre DR, Slayter HS. Type VI collagen of the intervertebral disc. Biochemical and electron-microscopic characterization of the native protein. *Biochem J*. 1987;**248**(2):373–381.
38. Smeriglio P, Dhulipala L, Lai JH, et al. Collagen VI enhances cartilage tissue generation by stimulating chondrocyte proliferation. *Tissue Eng Part A*. 2015;**21**(3-4):840–849.
39. Martinelli-Boneschi F, Colombi M, Castori M, et al.; INGI Network. COL6A5 variants in familial neuropathic chronic itch. *Brain*. 2017;**140**(3):555–567.
40. Gara SK, Grumati P, Urciuolo A, et al. Three novel collagen VI chains with high homology to the alpha3 chain. *J Biol Chem*. 2008;**283**(16):10658–10670.
41. Wang X, Pandey AK, Mulligan MK, et al. Joint mouse-human phenome-wide association to test gene function and disease risk. *Nat Commun*. 2016;**7**:10464.
42. Beaulieu M, Lévesque E, Hum DW, Bélanger A. Isolation and characterization of a novel cDNA encoding a human UDP-glucuronosyltransferase active on C19 steroids. *J Biol Chem*. 1996;**271**(37):22855–22862.
43. Sten T, Bichlmaier I, Kuuranne T, Leinonen A, Yli-Kauhaluoma J, Finel M. UDP-glucuronosyltransferases (UGTs) 2B7 and UGT2B17 display converse specificity in testosterone and epitestosterone glucuronidation, whereas UGT2A1 conjugates both androgens similarly. *Drug Metab Dispos*. 2009;**37**(2):417–423.
44. Zhu AZ, Cox LS, Ahluwalia JS, et al. Genetic and phenotypic variation in UGT2B17, a testosterone-metabolizing enzyme,

is associated with BMI in males. *Pharmacogenet Genomics*. 2015;**25**(5):263–269.
45. Swanson C, Mellström D, Lorentzon M, et al. The uridine diphosphate glucuronosyltransferase 2B15 D85Y and 2B17 deletion polymorphisms predict the glucuronidation pattern of androgens and fat mass in men. *J Clin Endocrinol Metab*. 2007;**92**(12):4878–4882.
46. Giroux S, Bussières J, Bureau A, Rousseau F. UGT2B17 gene deletion associated with an increase in bone mineral density similar to the effect of hormone replacement in postmenopausal women. *Osteoporos Int*. 2012;**23**(3):1163–1170.
47. Yang TL, Chen XD, Guo Y, et al. Genome-wide copy-number-variation study identified a susceptibility gene, UGT2B17, for osteoporosis. *Am J Hum Genet*. 2008;**83**(6):663–674.
48. Grant DJ, Chen Z, Howard LE, et al. UDP-glucuronosyltransferases and biochemical recurrence in prostate cancer progression. *BMC Cancer*. 2017;**17**(1):463.
49. Vanderschueren D, Vandenput L, Boonen S, Lindberg MK, Bouillon R, Ohlsson C. Androgens and bone. *Endocr Rev*. 2004;**25**(3):389–425.
50. Mohamad NV, Soelaiman IN, Chin KY. A concise review of testosterone and bone health. *Clin Interv Aging*. 2016;**11**:1317–1324.
51. Clarke BL, Khosla S. Androgens and bone. *Steroids*. 2009;**74**(3):296–305.
52. Kameda T, Mano H, Yuasa T, et al. Estrogen inhibits bone resorption by directly inducing apoptosis of the bone-resorbing osteoclasts. *J Exp Med*. 1997;**186**(4):489–495.
53. Robinson LJ, Yaroslavskiy BB, Griswold RD, et al. Estrogen inhibits RANKL-stimulated osteoclastic differentiation of human monocytes through estrogen and RANKL-regulated interaction of estrogen receptor-alpha with BCAR1 and Traf6. *Exp Cell Res*. 2009;**315**(7):1287–1301.
54. van Coeverden SC, Netelenbos JC, de Ridder CM, Roos JC, Popp-Snijders C, Delemarre-van de Waal HA. Bone metabolism markers and bone mass in healthy pubertal boys and girls. *Clin Endocrinol (Oxf)*. 2002;**57**(1):107–116.
55. Phillip M, Maor G, Assa S, Silbergeld A, Segev Y. Testosterone stimulates growth of tibial epiphyseal growth plate and insulin-like growth factor-1 receptor abundance in hypophysectomized and castrated rats. *Endocrine*. 2001;**16**(1):1–6.
56. Weise M, De-Levi S, Barnes KM, Gafni RI, Abad V, Baron J. Effects of estrogen on growth plate senescence and epiphyseal fusion. *Proc Natl Acad Sci U S A*. 2001;**98**(12):6871–6876.
57. Eriksson N, Tung JY, Kiefer AK, et al. Novel associations for hypothyroidism include known autoimmune risk loci. *Plos One*. 2012;**7**(4):e34442.
58. Kim HY, Mohan S. Role and mechanisms of actions of thyroid hormone on the skeletal development. *Bone Res*. 2013;**1**(2):146–161.
59. Rose SR. Isolated central hypothyroidism in short stature. *Pediatr Res*. 1995;**38**(6):967–973.
60. Sneha LM, Thanasegarapandian K, Paramasivam V, Scott JX. Short stature and an interesting association. *Indian J Hum Genet*. 2013;**19**(1):101–103.
61. Zhang Y, Xu YZ, Sun N, et al. Long noncoding RNA expression profile in fibroblast-like synoviocytes from patients with rheumatoid arthritis. *Arthritis Res Ther*. 2016;**18**(1):227.
62. Gieger C, Radhakrishnan A, Cvejic A, et al. New gene functions in megakaryopoiesis and platelet formation. *Nature*. 2011;**480**(7376):201–208.
63. Nürnberg ST, Rendon A, Smethurst PA, et al.; HaemGen Consortium. A GWAS sequence variant for platelet volume marks an alternative DNM3 promoter in megakaryocytes near a MEIS1 binding site. *Blood*. 2012;**120**(24):4859–4868.
64. He M, Xu M, Zhang B, et al. Meta-analysis of genome-wide association studies of adult height in East Asians identifies 17 novel loci. *Hum Mol Genet*. 2015;**24**(6):1791–1800.
65. Chang L, Zhang Z, Yang J, McLaughlin SH, Barford D. Atomic structure of the APC/C and its mechanism of protein ubiquitination. *Nature*. 2015;**522**(7557):450–454.
66. Chang LF, Zhang Z, Yang J, McLaughlin SH, Barford D. Molecular architecture and mechanism of the anaphase-promoting complex. *Nature*. 2014;**513**(7518):388–393.
67. Wittke I, Wiedemeyer R, Pillmann A, Savelyeva L, Westermann F, Schwab M. Neuroblastoma-derived sulfhydryl oxidase, a new member of the sulfhydryl oxidase/Quiescin6 family, regulates sensitization to interferon gamma-induced cell death in human neuroblastoma cells. *Cancer Res*. 2003;**63**(22):7742–7752.
68. Fujihara J, Takeshita H, Kimura-Kataoka K, et al. Replication study of the association of SNPs in the LHX3-QSOX2 and IGF1 loci with adult height in the Japanese population; wide-ranging comparison of each SNP genotype distribution. *Leg Med (Tokyo)*. 2012;**14**(4):205–208.
69. Schaeffer E, Vigneron M, Sibler AP, Oulad-Abdelghani M, Chatton B, Donzeau M. ATF7 is stabilized during mitosis in a CDK1-dependent manner and contributes to cyclin D1 expression. *Cell Cycle*. 2015;**14**(16):2655–2666.
70. N'Diaye A, Chen GK, Palmer CD, et al. Identification, replication, and fine-mapping of Loci associated with adult height in individuals of African ancestry. *Plos Genet*. 2011;**7**(10):e1002298.
71. Houstěk J, Andersson U, Tvrdík P, Nedergaard J, Cannon B. The expression of subunit c correlates with and thus may limit the biosynthesis of the mitochondrial F0F1-ATPase in brown adipose tissue. *J Biol Chem*. 1995;**270**(13):7689–7694.
72. Deng FY, Dong SS, Xu XH, et al. Genome-wide association study identified UQCC locus for spine bone size in humans. *Bone*. 2013;**53**(1):129–133.
73. Sanna S, Jackson AU, Nagaraja R, et al. Common variants in the GDF5-UQCC region are associated with variation in human height. *Nat Genet*. 2008;**40**(2):198–203.
74. Plachy L, Strakova V, Elblova L, et al. High prevalence of growth plate gene variants in children with familial short stature treated with GH. *J Clin Endocrinol Metab*. 2019;**104**(10):4273–4281.